Electronic Supplementary Material (ESI) for Soft Matter
This journal is © The Royal Society of Chemistry 2013

Supplementary materials for

"The stability of thin polymer films as controlled by changes in uniformly sputtered gold"

G. Amarandei, C. O'Dwyer, A. Arshak and D. Corcoran

1.Instability development in a thin polymer film

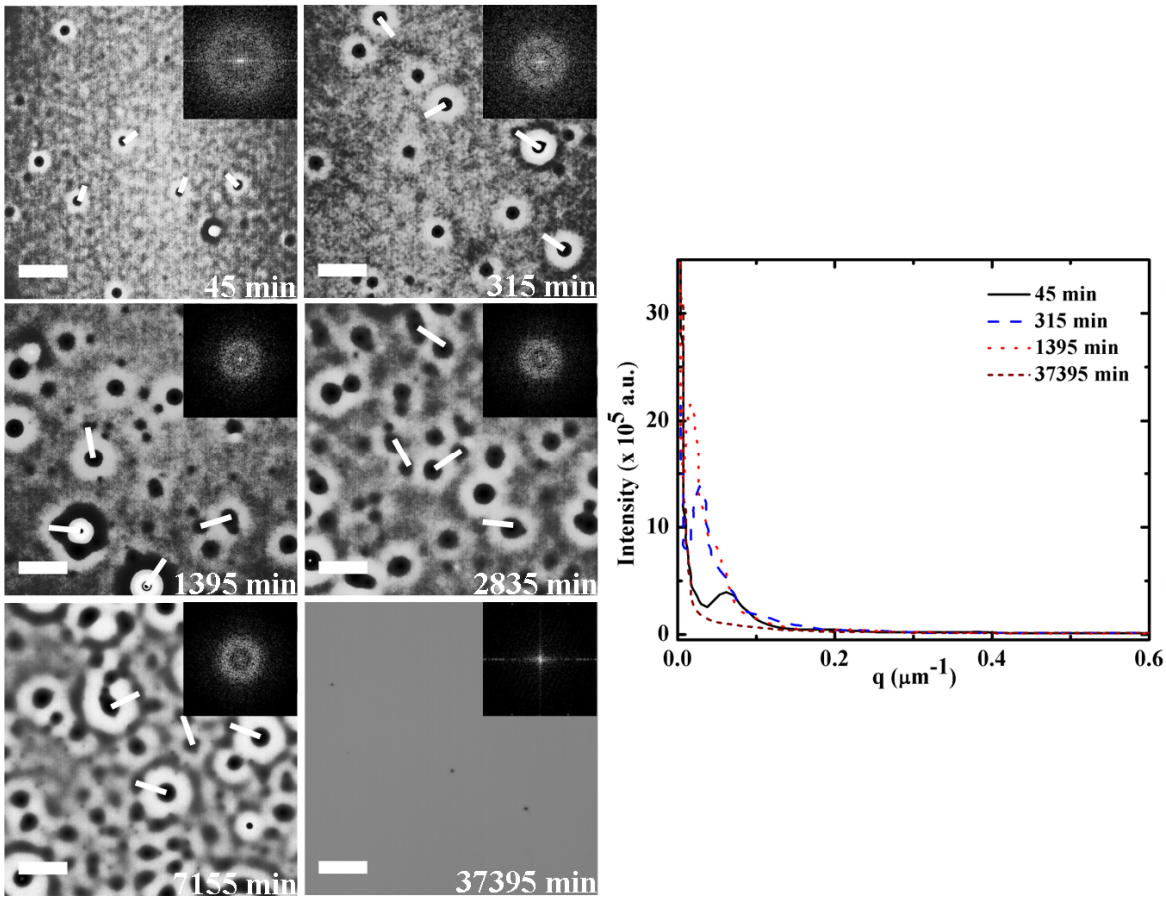

Figure S1. Optical micrographs of the PS10 film (h_{PS} = 26 nm, h_{Au} = 3 nm) at indicated time steps. Insets show the corresponding FFTs of these images. The size of the thin white lines included in the image is equal to the measured wavelength at a time step (**Figure 4**). The white (thick) scale bars represent 50 μm. The FFT profiles for 45, 315, 1395 and 37395 min are also presented. These time steps were chosen to show the initial increase in the wavelength (i.e. the decrease in the wavenumber q) as from 1395 to 7155 min the wavelength remains relatively constant. The FFT profile at t = 37395 min was included to show that the film returns to being flat.

This journal is © The Royal Society of Chemistry 2013

Optical images showing the development of the polymer instability in the h_{Au} = 3 nm covered sample are presented in **Figure S1** for several experimental time steps. The FFTs of these images are included as insets. A single large ring can be seen in the FFT at 45 min. The diameter of the ring decreases from 45 to 1395 min and the corresponding wavelength increases in time (see also **Figure 4**). Thereafter, up to t = 7155 min, the ring diameter and wavelength are approximately constant within experimental error (10%). Lines corresponding to the wavelengths are included at each time step to illustrate the development of the instability.

2. Au aggregation and rearrangement

The particle evolution with heating as seen in the original SEM images (Figure S2) and in their binary versions (Figure S3) show that as the particles diffuse and aggregate their areal coverage decreases, but their distribution is maintained homogenously independent of the SEM images being acquired on the peaks or within the troughs of the surface instability.

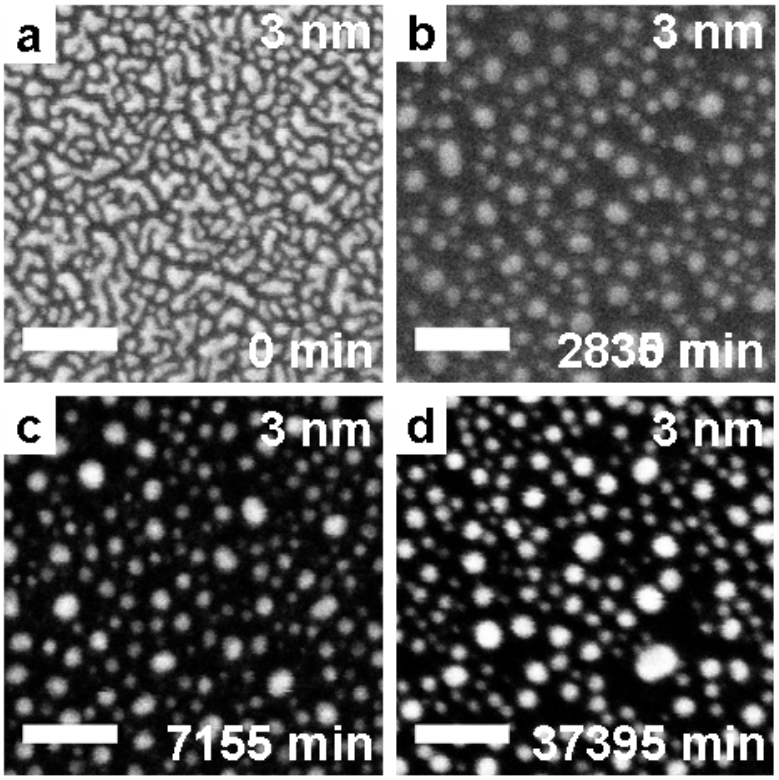

Figure S2. Original SEM images for the h_{Au} = 3 nm Au sample at (a) t = 0 min, (b) t = 2835 min, (c) t = 7155 min and (d) t = 37395 min. The scale bar represents 50 nm.

This journal is © The Royal Society of Chemistry 2013

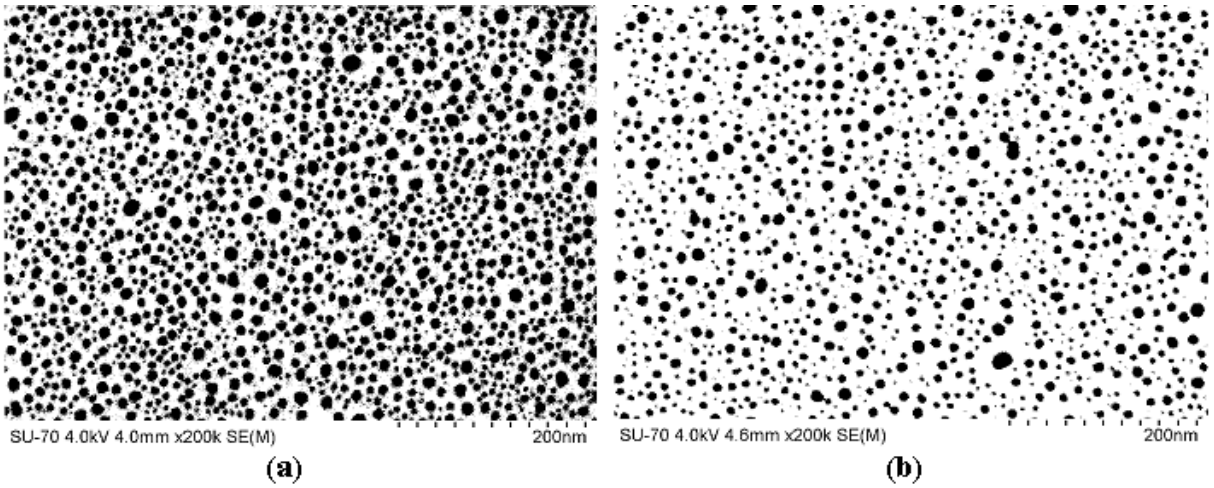

Figure S3. Binary SEM images for the h_{Au} = 3 nm Au sample at (a) t = 7155 min and (b) t = 37395 min.

The particle number density, mean diameter and form shape factor are presented as a function of experimental heating time in **Figure S4**. The particle densities for all samples decrease marginally from early times (45 min to 315 min) to later times (1395 min to 7155 min). At t = 37395 min there is a significant decrease in the particle densities for the h_{Au} = 1 nm and 2 nm samples and a smaller reduction is also seen at t = 37395 min for the h_{Au} = 3 nm, most likely a consequence of the slower movement of the initially larger particles. For h_{Au} = 0.3 nm, coalescence is retarded due to the larger spacing between particles, and this is apparent in the unchanged particle density between t = 7155 and 37395 min. For h_{Au} = 3 nm, the mean diameter increases marginally up to t = 7155 min as aggregation takes place. As Au NPs diffuse, they reorganize and agglomerate into bigger clusters. Particles in a cluster initially connect via a "neck" [1] but due to resolution limits the clusters are seen using SEM as single particles with increasing mean diameter. Between t = 45 min and t = 2835 min the form shape factor oscillates between becoming more and less spherical, but the tendency to a less spherical shape dominates. Particle rearrangement competes with aggregation as the Au seeks to minimize its free energy, but aggregation dominates as the particle diameter increases in time. As larger particles form they diffuse more slowly on the film surface due to larger adhesion to the substrate.[1 – 4] Therefore, aggregation slows at later times t > 2835 min and the clusters rearrange into spheres leading to an increase in the form shape factor [4] and decreased diameter at t = 37395 min.

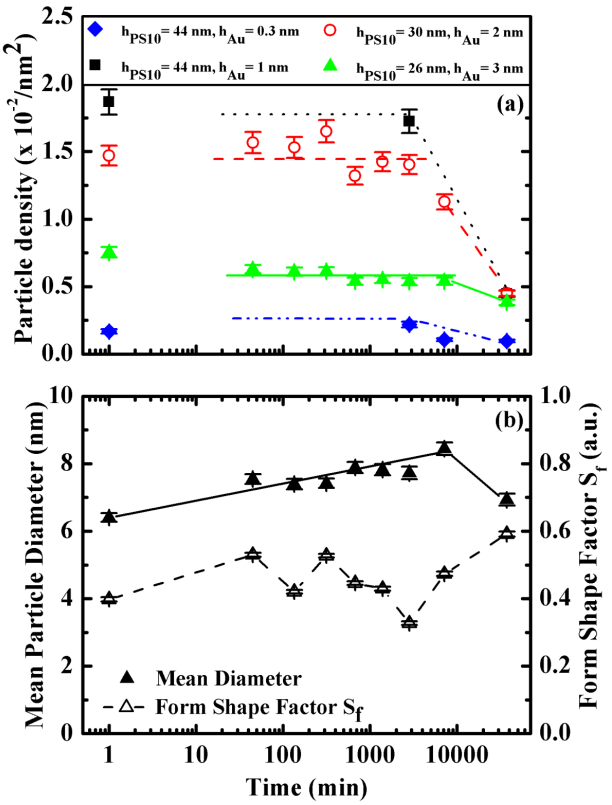

Figure S4. The particle density (a), mean diameter and form shape factor (b) of the Au NPs after heating as a function of experimental time. NP mean diameter and form shape factor are presented for the sample with Au film thickness of h_{Au} = 3 nm on h_{PS} = 26 nm.

During the deposition it is expected that a small amount of Au will diffuse into the polymer thin film[5] to a certain distance from its surface. Kaune *et al.*[5a] reported using X-ray reflectivity that for a Au layer (h_{Au} = 25 nm) deposited on poly (N-vinylcarbazole) (PVK) an amount of less than 0.1 monolayer is incorporated into the polymer film. Such a layer will be formed by Au single atoms or very small clusters, but their measurements could not give precise information on this aspect or on the temporal progress of the penetration process.[5a] In a specific designed study Ferreira *et al*[5b] used cathodic arc plasma ion implantation to place Au nanoparticles at ~ 4 nm below the air interface of a poly(methyl-methacrylate) (PMMA) thin film. This was done using a filtered cathodic vacuum arc technique where ions are highly energetic.

In the study here, however, the maximum thickness for which a discontinuous NP layer was investigated is h_{Au} = 3 nm and was obtained under "classic" deposition conditions. Therefore,

This journal is © The Royal Society of Chemistry 2013

it can be expected that the amount of Au implanted below the interface will be smaller than the 0.1 of a monolayer obtained by Kaune *et al*.[5a] Also, once the polymer is heated, it is expected that the atoms and small clusters[5a] will be the first to diffuse and aggregate with the bigger particles (by the end of the first experimental time step) as they will have the largest diffusion coefficients.[1 – 4] Therefore, this embedded Au is not considered in the presented model. However, further studies using X-ray reflectivity will be performed in the future in order to determine this amount of Au and to incorporate its contribution (if any) to the film stability.

3. van der Waals potential for Au NP

The van der Waals potential between a Au particle and the underlying layers[1], namely for the Si/SiO_x/PS/AuNP/air system can be written as:

$$\Phi_{AuNP}(h,R_p) = -\frac{A_{air/Au/poly}}{6}\left(\frac{R_p}{h}+\frac{R_p}{h+2R_p}+\log\frac{h}{h+2R_p}\right)$$
$$+\frac{2A_{air/Au/poly}-A_{air/Au/SiOx}-A_{air/Au/Si}}{6}\left(\frac{R_p}{h+h_{SiOx}}+\frac{R_p}{h+h_{SiOx}+2R_p}+\log\frac{h}{h+h_{SiOx}+2R_p}\right)$$

where h is the thin polymer thickness, h_{SiOx} is the natural SiO_x layer thickness, and the $A_{air/Au/poly}$ Hamaker constant is counted twice as the interactions with both Si and SiO_x layers are considered.

Name	Without chemical changes t = 0 min (J)	With chemical changes t = 37395 min (J)
$A_{air/PS/Si}$	-9.76×10^{-20}	-9.27×10^{-20}
$A_{air/PS/SiOx}$	$+5.31\times10^{-21}$	-3.17×10^{-21}
$A_{air/Au/PS}$	$+1.21\times10^{-19}$	$+1.30\times10^{-19}$
$A_{air/Au/Si}$	-1.00×10^{-20}	-1.00×10^{-20}
$A_{air/Au/SiOx}$	$+1.26\times10^{-19}$	$+1.26\times10^{-19}$

Table S1. Hamaker constants used to calculate the potential, stability (without and with thinning) and wavelength (i.e. **Figures 4**, **Figure 7a** and **b**) and the Hamaker constants used to calculate the stability after correction for thinning and chemical damage (**Figure S5** and **S7**)

This journal is © The Royal Society of Chemistry 2013

The Hamaker constants (assuming no chemical damage) used in the paper are presented in the first column of **Table S1**. All Hamaker constants were calculated using Lifshitz theory following the procedure presented in [6]. The refractive indices used were n_{PS} = 1.60, n_{Si} = 4.11, n_{SiOx} = 1.46, with corresponding UV absorption frequencies of 2.3, 1.0 and 3.24 × 10^{15} Hz. The plasma frequency for Au was taken as 2.18 × 10^{15} Hz.

4. Polymer film chemical integrity and possible effects on film stability

As an extended period of heating or annealing time is used in the studies presented here, and since the polymer films are heated in air, physical and chemical changes that might take place in the film and their influence on the formation of the polymer instability are considered. Thinning is found to occur, possibly due to polymer evaporation and/or polymer densification as a result of adhesion to the Au.[7,8] After 37395 min of heating, a reduction of 27, 27, 25 and 22% with respect to the initial thicknesses is measured for the samples with nominal Au deposits of 0.3, 1, 2 and 3 nm respectively. Therefore, the stability curves presented in **Figure 7a** are recalculated on the basis of the reduced thicknesses (see **Figure S5)**. The effect of a lowered film thickness is to raise the stability curve that separates unstable from metastable regimes. Importantly, those points predicted and observed to be unstable, and those points predicted and observed to be metastable remain so, after allowing for the effect of thinning.

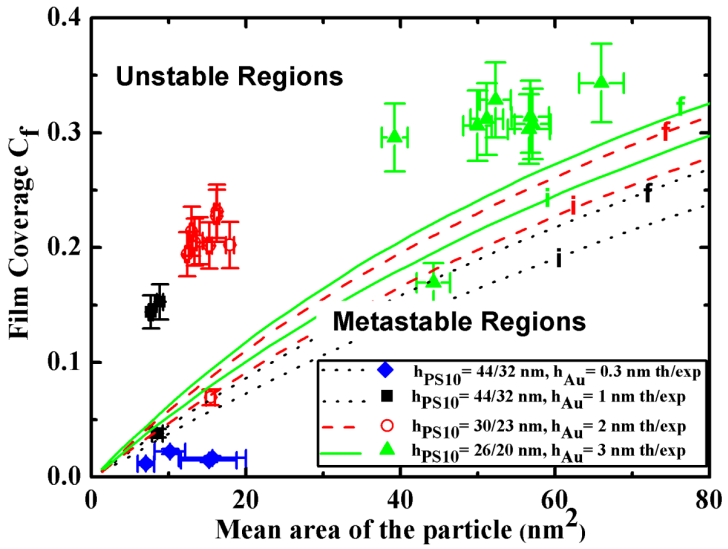

Figure S5. Phase diagram of the transition from unstable to metastable regimes before (labeled *i*) and after (labeled *f*) polymer evaporation (film thinning)

This journal is © The Royal Society of Chemistry 2013

The chemical integrity of the polymer film surface is examined using XPS analysis. This is a well established method that can describe the degradation of a thin polymer film surface during UV,[9] thermal[10–12] or plasma[13, 14] treatment. As the h_{Au} = 1 nm sample has the lowest Au coverage of those samples exhibiting a spinodal instability and therefore the greatest polymer exposure, one can expect that the thermal degradation will be most pronounced for this sample.

The high resolution C1s spectra of the h_{Au} = 1 nm are presented for t = 0 min and t = 37395 min in **Figure S6** and the corresponding concentrations measured from the individual peaks are detailed in **Table S2**. Prior to heating (t = 0 min) oxygen is present at the surface as a result of the Au deposition by plasma sputtering.[14] The peak at 284.8 eV observed here can be identified with the 285 eV peak comprised of aliphatic and aromatic components.[13,14] The associated C-C and C-H bonds together with the separate $\Pi - \Pi^*$ shake up satellite at 291.6 eV (indicative of aromatic chemistry) are together characteristic of the PS film. Peaks corresponding to C-OR/C-OH, C=O, O-C=O are in contrast characteristic of degradation of the polymer film surface. The signature of PS, as measured by the peaks at 284.8 eV (C-C and C-H) and 291.6 eV ($\Pi - \Pi^*$ shake up satellite) compared to the overall C1s signal diminishes as a result of heating from 86.7% to 84.6%, that is a relative negligible reduction or degradation of 2%. A key indicator of PS degradation is also the disappearance of the $\Pi - \Pi^*$ shake up satellite peak,[13, 14] as the aromatic structure of PS decomposes (see also Ref. [14] and references therein). This signature is not observed; in fact the strength of the peak actually increases. The increase can be attributed to the fresh exposure of polymer as the gold coalesces and restructures. From the survey XPS spectra the Au4f signal decreases by 60% from t = 0 min to 37395 min, a result of the rearrangement and coalescence of Au NPs described above. The reduction is consistent with measurements from SEM observation that show Au coverage reduction on the same sample of ~ 70% (see **Figure 5b**). Overall therefore, degradation does occur during the annealing time, but chemical changes in the PS appear nevertheless to be relatively small.

This journal is © The Royal Society of Chemistry 2013

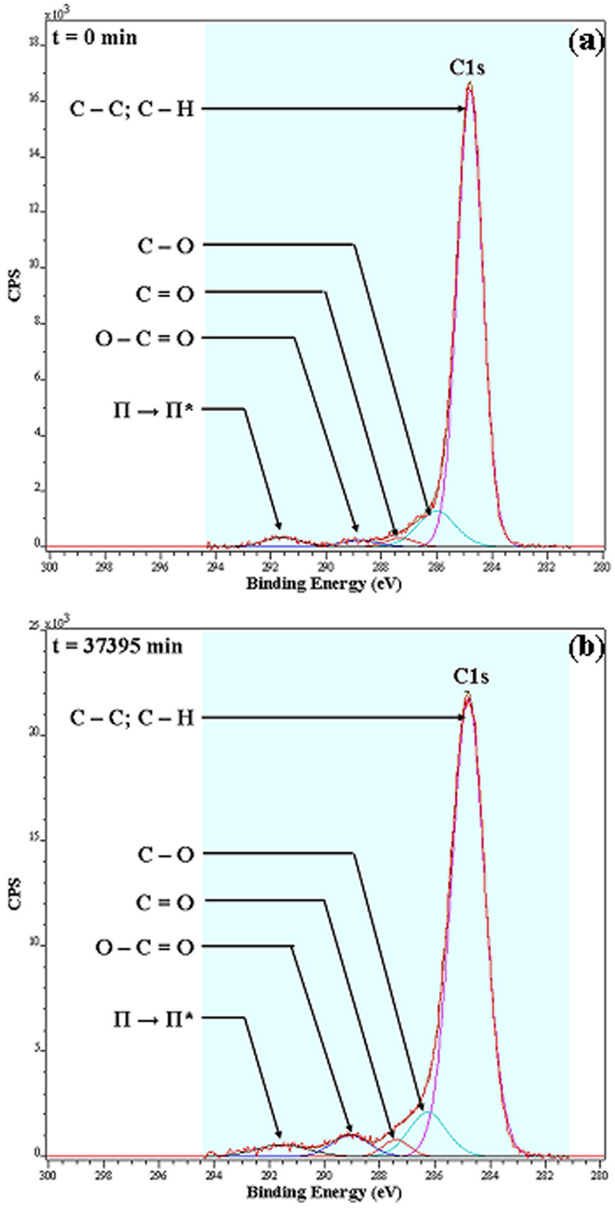

Figure S6. C1s photoelectron peaks (a) before (t = 0 min) and (b) after (t = 37395 min) heating. The spectra were analyzed using Casa XPS software and assignments made using the NIST X-ray photoelectron spectroscopy database, version 3.5. The minimum number of peaks was used for fitting the spectra.

The presence of C-OR/C-OH, C=O and O-C=O functionalities might alter the polymer film surface tension. It can be estimated that at most, there could be an ~ 8% reduction in PS surface tension, assuming chain scission at higher M_w applies[15, 16] to the lower M_w studies here

This journal is © The Royal Society of Chemistry 2013

and given the weak dependence of surface tension on M_w.[17] The incorporation of oxygen might additionally or alternatively reduce film viscosity if again caused by chain scission.[18] In fact, based on the work of McNeill *et al.* [15] it is not at all clear that chain scission can take place in thin films at the low M_w (10k) and working temperatures (170 ºC) used in the work here. Moreover, it was recently shown that the thermal stability of PS-Au microspheres is slightly higher than that of pure PS.[12] Therefore Au NPs could obstruct the decomposition route during thermal treatment, inducing its shift towards higher temperatures.[12] Regardless, even if scission takes place, such functionalities cannot cause the observed presence and then absence of the instability observed experimentally; that depends solely on Φ_{hh} which is independent of both parameters. The model equation for the growth rate β presented in this study shows that a reduced film viscosity and therefore increased mobility can lead to faster growth. So as a result the instability might be observed more rapidly, but this is secondary to the film already being unstable. The growth rate equation and equation 2 predict that the effect of changing surface tension is to modify the wavelength and growth rate, but as the surface tension is dominated by the presence of Au, the influence of such degradation is likely to be marginal.

The oxygen content at t = 37395 min can be estimated based on the C-OR/C-OH, C=O, O-C=O peaks in the C1s high resolution spectra, and the oxygen signal from the XPS survey spectra to lie in the range 13-22%. Choosing the upper limit to reflect the greatest degradation, and assuming that this is the oxygen concentration over the XPS measurement depth of ~ 4.7 nm, the refractive index changes in this PS layer[19] and the refractive index in the compound PS film are calculated.

Revised Hamaker constants are then recalculated for the present model on this basis (presented together with the original ones in **Table S1**). Allowing for physical changes i.e. thinning by using the final film thicknesses, and chemical changes using the revised Hamaker constants, the stability curves are regenerated (presented together with the experimental data in the phase diagram in **Figure S7)**. In comparison with **Figure 7a**, those points predicted originally as being unstable, and those points predicted to be in the metastable regime remain so. It is evident that a reduction in Au coverage dominates over chemical and physical changes in determining the polymer film stability. Therefore, it can be concluded that a reduction in Au coverage as a result of NP rearrangement and coalescence drives the thin polymer film from the unstable to metastable regime.

Name	t = 0 min		t = 37395 min	
	Energy (eV)	Conc. (%)	Energy (eV)	Conc. (eV)
C-C, C-H	284.8	84.2	284.8	81.3
C-OR, C-OH	286.0	9.8	286.3	8.8
C=O	287.3	1.8	287.5	2.4
O-C=O	288.8	1.7	289.1	4.3
$\Pi \rightarrow \Pi^*$	291.6	2.5	291.6	3.3

Table S2. Chemical assignments from high resolution spectrum of C1s signal at t = 0 min and after 37395 min heating. The concentrations expressed as a percentage of the C1s signal at respective times are given. At the take-off angle of 90º (i.e. normal to the surface) the estimated analysis depth is ~ 4.7 nm.

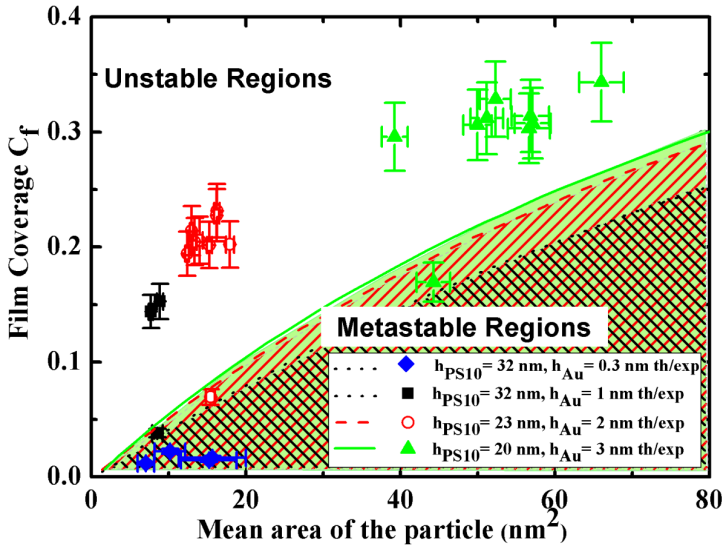

Figure S7. Phase diagram of the transition from unstable to metastable regimes allowing for thinning and chemical degradation

This journal is © The Royal Society of Chemistry 2013

References:

[1] M. Jose-Yacaman, C. Gutierrez-Wing, M. Miki, D. Q. Yang, K. N. Piyakis, and E. Sacher, *J. Phys. Chem. B*., 2005, **109**, 9703

[2] W.A. Lopes and H. M. Jaeger, *Nature*, 2001, **414**, 735

[3] W. A. Lopes, *Phys. Rev. E.*, 2002, **65**, 031606

[4] X. Jia, J. Listak, V.Witherspoon, E. E. Kalu, X. Yang, and M. R.Bockstaller, *Langmuir*, 2010, **26**, 12190

[5] (a) G. Kaune, M.A. Ruderer, E. Metwalli, W. Wang, S. Couet, K. Schlage, R. Röhlsberger, S. V. Roth, and P. Müller-Buschbaum, *ACS Appl. Mater. Interfaces*, 2009, **1**, 353; (b) J. Ferreira, F.S. Teixeira, A.R. Zanatta, M.C. Salvadori, R. Gordon and O.N. Oliveira Jr, *Phys.Chem.Chem.Phys.*, 2012, **14**, 2050

[6] J. Israelachvili, Intermolecular and Surface Forces (Academic Press, 1992)

[7] S. Napolitano and M. Wubbenhorst, *Nature Communications*, 2011, **2**, 260

[8] T. Fu, U. Stimming, and C. Durning, *Macromolecules*, 1993, **26**, 3271

[9] A. Hozumi, H. Inagaki and T. Kameyana, *J. Colloid. Interface Sci.*, 2004, 278, 383

[10] J. Hao, S. Wua, C. A. Wilkie and J. Wang, *Polym. Degrad. Stab.*, 1999, 66, 81

[11] J. Wang, J. Du, H. Yao and C. A. Wilkie, *Polym. Degrad. Stab.*, 2001, 74, 321

[12] P. C. Chang, C. C. Tseng, J. L. Ou, W. H. Hwu and M. D. Ger, *Colloid. Polym. Sci.*, 2010, 288, 295

[13] D. Merche, C. Poleunis, P. Bertrand, M. Sferrazza and F. Reniers, *IEEE Trans. Plasma Sci.*, 2009, 37, 951

[14] E. H. Lock, D. Y. Petrovykh, P. Mack, T. Carney, R. G. White, S. G. Walton and R. F. Fernsler, *Langmuir*, 2010, 26, 8857

[15] I. C. McNeill and M. A. J. Mohammed, *Eur. Polym. J.*, 1972, 8, 975

[16] J. D. Peterson, S. Vyazovkin and C. A. Wight, *Macromol. Chem. Phys.* 2001, 202, 775

[17] K. K. Chee, *J. Appl. Polym. Sci.*, 1998, 70, 697

[18] G. Botelho, A. Queiro, A. Machado, P. Frangiosa and J. Ferreira , *Polym. Degrad. Stab.*, 2004, 86, 493

[19] G. V. Lubarsky, S. A. Mitchell, M. R. Davidson and R. H. Bradley, *Colloids and Surfaces A: Physicochem. Eng. Aspects*, 2006, 279 188195